

# Rational design of multifunctional framework materials for sustainable photocatalysis

Yingjie Fan and Wenbin Lin ⊚<sup>⊠</sup>

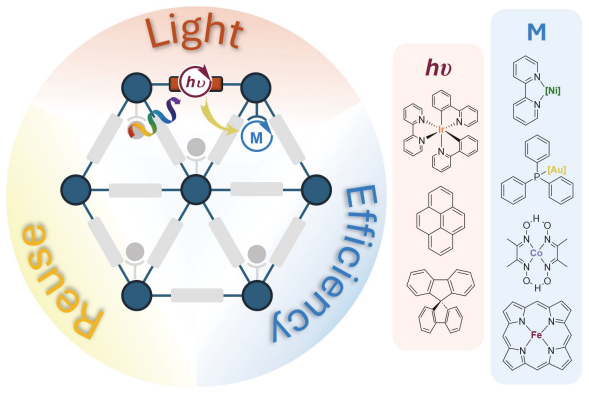
Department of Chemistry, The University of Chicago, Chicago, IL 60637, USA



Cite This: Carbon Future 2024, 1, 9200018



ABSTRACT: Photocatalysis harnesses photon energy to drive chemical reactions under mild conditions that would otherwise be thermodynamically uphill. Nature provides a blueprint for designing photocatalytic systems, as seen in photosynthesis, by assembling light-harvesting antenna complexes, electron transport chains, and catalytic enzymes to perform highly complex light-driven chemical syntheses. While methods leveraging the synergy between photosensitizers and catalytic complexes have been widely explored in photocatalysis, the hierarchical assembly of these components in material systems has been less studied. The emergence of framework materials, including metal-organic frameworks and covalent organic frameworks provides new opportunities for designing advanced photocatalysts based on these molecular



material platforms. This minireview focuses on the design of framework materials for sustainable photocatalysis. We will discuss the design of framework materials for artificial photosynthesis and several important organic transformations and highlight the advantages of these catalytic framework materials over their homogeneous counterparts. Framework material-based photocatalysts are readily recovered from reactions and reused in multiple reaction runs, further contributing to the development of sustainable photocatalytic processes.

KEYWORDS: metal-organic frameworks, covalent organic frameworks, artificial photosynthesis, photoredox catalysis

#### 1 Introduction

Harnessing sunlight energy has long been a global scientific pursuit. Photovoltaic (PV) cells, which convert sunlight into electricity, have become one of the most reliable and widely available sources of renewable energy¹. In contrast, chemical reactions heavily rely on metal catalysts and heat but have not benefitted from the advancements in PV technology. The direct conversion of sunlight energy into chemical energy hinges on the development of advanced photocatalytic systems.

Nature has provided a blueprint for designing photocatalytic systems through photosynthesis. In this process, a light-harvesting antenna molecule in photosystem II absorbs light and transports high-energy electrons through an electron transport chain. Another photon is absorbed by an antenna molecule in photosystem I in the chain, which uses electrons for nicotinamide adenine dinucleotide phosphate (NADPH) synthesis. Simultaneously, the holes

**Received:** August 5, 2024; **Revised:** September 12, 2024 **Accepted:** September 13, 2024

https://doi.org/10.26599/CF.2024.9200018

generated from light irradiation are used to drive water oxidation<sup>2, 3</sup>. Photosensitizers, electron shuttles, and catalytic species are hierarchically organized in photosynthetic systems to convert solar energy into chemical energy.

Studies combining photosensitizers and metal catalysts for chemical reactions began in 1970s. Water splitting and  $CO_2$  reduction were achieved by leveraging the synergy between  $Ru(bpy)_3^{2+}$  (bpy = 2,2′-bipyridine) photosensitizers and transition metal catalysts  $^4$ . The molecular design of photosensitizers and transition metal catalysts with higher reactivities has led to improved reaction performances  $^6$ . However, less attention has been given to designing assembled systems that enhance photocatalysis efficiency.

A straightforward design to enhance photocatalysis efficiency is to accelerate photoelectron transfer from photosensitizers. The basic theory of electron transfer has been extensively studied and described<sup>8</sup>. Pre-organizing a photosensitizer and an electron acceptor, typically a secondary catalytic center or reaction substrate, should reduce the kinetic barrier of electron transfer, thereby improving the overall reaction performance. Methods such as covalently linking a photosensitizer and a catalyst in a single molecule, designing heterogeneous co-catalysts, or developing hybrid catalysts, have demonstrated the potential of the preorganization strategy and significantly increased the efficiency of



Address correspondence to Wenbin Lin, wenbinlin@uchicago.edu



artificial photosynthesis<sup>9–13</sup>. Among them, assembling catalysts within a supramolecular host provides a method of achieving precise molecular control in the system, also allowing for detailed characterization.

Framework materials, including metal-organic frameworks (MOFs)<sup>14</sup> and covalent organic frameworks (COFs)<sup>15</sup> serve as ideal supramolecular material platforms for designing photocatalytic systems<sup>16, 17</sup>. Framework materials are crystalline porous materials constructed through periodic bonding of building blocks. MOFs are built via coordination between metals and organic ligands, whereas COFs are formed through covalent bonding between the building blocks. Since the first report on MOFs, prefunctionalization of organic ligands has been employed to install catalytic moieties<sup>18-21</sup>. More recently, post-modification of open metal sites has been explored to introduce additional catalytic functions<sup>22-26</sup>. This same strategy can be applied to COFs to orthogonally integrate different functionalities in the building units. Consequently, photosensitizing and catalytic components can be pre-organized hierarchically in framework materials to accelerate photoelectron transfer.

The hierarchical integration of photosensitizing and catalytic components can be characterized by both direct and indirect methods. Direct methods, such as powder X-ray diffraction (PXRD) and X-ray absorption spectroscopy (XAS), analyze the structure and chemical composition of framework materials without destroying the samples. Indirect methods use chemical reagents to digest framework materials into separate building blocks, which are then characterized with quantitative solution-based techniques such as nuclear magnetic resonance spectroscopy (NMR), ultraviolet–visible (UV–vis) light spectroscopy, and inductively coupled plasma-mass spectrometry (ICP-MS).

Metal-organic layers (MOLs), a two-dimensional (2D) version of MOFs, offer additional advantages as photocatalysts, including larger surface areas and more modifiable sites. MOLs were first reported in 2016 as fully dispersible materials with modifiable surface sites equivalent in number to their bridging ligands<sup>27</sup>. Since then, MOLs have been widely studied as site-isolated catalysts and synergistic catalysts. The first reported COF had a 2D structure<sup>15</sup>, but 2D COFs tend to stack along the third dimension, which compromises the accessibility of the active sites to reactants when compared to MOLs. 2D COFs have also been examined in a variety of photocatalytic reactions<sup>28–31</sup>.

In this minireview, assembled photocatalytic systems based on framework materials with pre-functionalized photosensitizing linkers and post-synthetically introduced synergistic catalysts are discussed (Fig. 1). Significant enhancements in reaction efficiency are observed in framework material-catalyzed artificial photosynthesis and various organic transformations compared to those catalyzed by simple mixtures of the corresponding components. The tunable and well-defined active sites in framework materials allow their rational design to optimize photocatalytic efficiency, thus providing a basis for achieving sustainable photocatalysis. Framework materials have also been demonstrated to be stable and reusable under catalytic conditions, further contributing to a more sustainable photocatalytic process.

## 2 Monolayered MOFs for artificial photosynthesis

As previously discussed, photosensitizers, electron transfer chains,

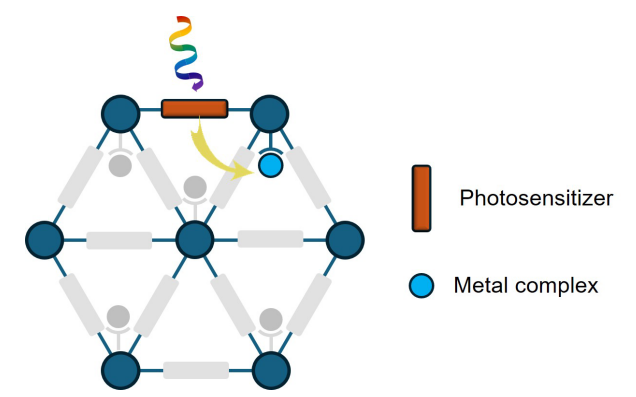


Fig. 1. Framework materials for sustainable photocatalysis.

and catalytic enzymes are intricately organized to achieve natural photosynthesis. Numerous photocatalytic systems have been developed to mimic this feature of natural photosynthesis <sup>10, 32–36</sup>. However, achieving effective synergy in artificial photosynthesis is challenging without precise control over the assembly and molecular structures of the photosensitizers and catalysts. The structural features of framework materials have allowed the design of efficient catalysts for artificial photosynthesis <sup>37–39</sup>. In this section, we present a photocatalytic system based on MOLs, monolayered MOFs, for artificial photosynthesis with enhanced activities through rational design <sup>40</sup>.

Photosensitizing linkers, specifically linear dicarboxylic acids based on the bis(phenylpyridine)iridium(bipyridine) moiety (Ir-PS), connect  $Hf_{12}$ -based SBUs to form MOLs as hexagonal nanoplates. For water oxidation reactions, the surface of these nanoplates was modified via carboxylate exchange with water oxidation catalysts, *i.e.* (pentamethylcyclopentadienyl)iridium(bipyridine) complexes ([Ir]), and amino acids (AAs) (Fig. 2a). The AAs account for around 90% of the surface sites, mimicking the secondary coordination environments known in the active sites of natural enzymes. Similarly, the MOL for  $CO_2$  reduction was constructed with Ir-PS, hemin ([Fe] as a  $CO_2$  reduction catalyst), and AAs (Fig. 2a).

The reactivities of MOLs were systematically optimized through screening AAs to tune the secondary environments of the catalytic centers. For example, a library of MOLs for water oxidation was created by loading 20 proteinogenic AAs onto the surface of the MOLs. Examination of their reactivities towards photocatalytic water oxidation, using sacrificial oxidant  $K_2S_2O_8$ , revealed a catalytic efficiency trend correlated to the oxidation potentials of the AA side chains (Fig. 2b). Glutamine (Q) and asparagine (N), which contain amide side chains, were found to enhance the reaction most effectively. Consequently, an artificial ligand featuring an *N*-aryl amide group, Am-Cl, was designed and integrated into the MOL, resulting in a turnover number (TON) of 1440 in 6 h.

AA optimization for  $\mathrm{CO}_2$  photoreduction revealed two mechanisms that increase reaction rates (Fig. 2c). AAs with acidic side chains accelerate  $\mathrm{CO}_2$  reduction via a proton-coupled electron transfer (PCET) process. AAs with amide side chains function as hydrogen bond donors, stabilizing the  $\mathrm{CO}_2$  radical anion intermediate and thereby lowering the reaction barrier. The hydrogen bonding effect offers a more significant enhancement. Consequently, an artificial ligand featuring a urea group, Ur, was designed and integrated into the MOL, achieving a TON of 1146 in 6 h.





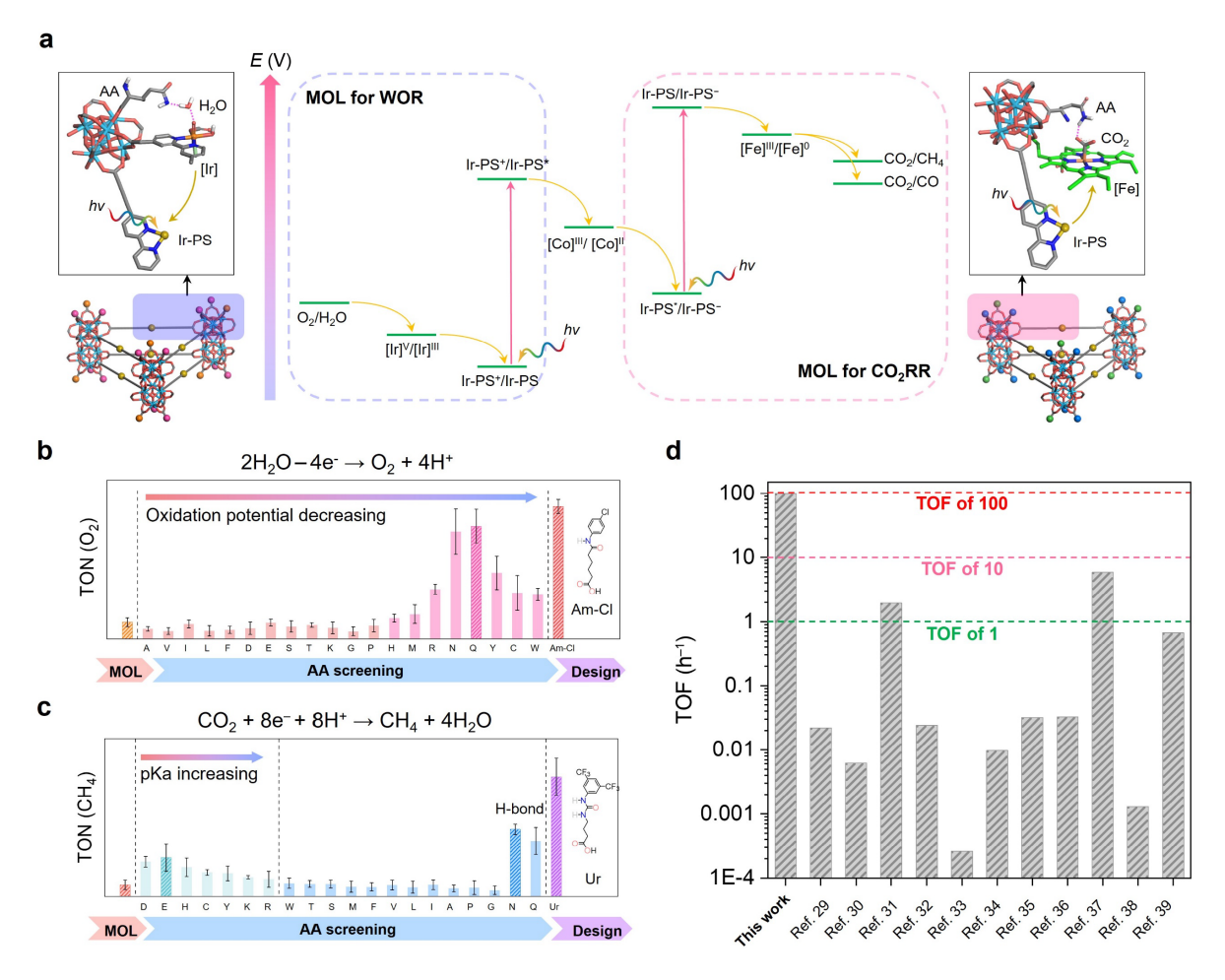


Fig. 2. Design of monolayered metal-organic frameworks for artificial photosynthesis. a, Z-scheme of artificial photosynthesis catalyzed by two MOL-based catalysts. b, Optimization of secondary coordination provided by amino acids in water oxidation half reaction. c, Optimization of secondary coordination provided by amino acids in CO<sub>2</sub> reduction half reaction. d, Summary of activities for photocatalytic conversion of CO<sub>2</sub> to CH<sub>4</sub> by the MOL and previously reported catalysts. Reproduced with permission from Ref.<sup>40</sup>, © Springer Nature 2022.

Integration of photosensitizers and catalytic complexes in the MOLs significantly enhances their reaction efficiency compared to corresponding homogeneous catalysts. For instance, the MOL designed for water oxidation catalyzed the reaction 10 times faster than a mixture of Ir-PS, [Ir], and Am-Cl. Similarly, the MOL designed for CO<sub>2</sub> reduction catalyzed the reaction 28 times faster (based on CH<sub>4</sub> production) than a mixture of Ir-PS, [Fe] and Ur. In subsequent studies, a full reaction without sacrificial reagents was explored using an electron mediator, Co(bpy)<sub>3</sub>Cl<sub>2</sub>([Co]), to couple catalytic cycles of water oxidation with CO<sub>2</sub> reduction, mimicking the electron transport chain in natural photosynthesis (Fig. 2a). This integrated photocatalytic system achieved an overall turnover frequency (TOF) of 98 h<sup>-1</sup> for CO<sub>2</sub> to CH<sub>4</sub> conversion, with a quantum yield of 1.1% at 350 nm, significantly outperforming other reported systems at the time (Fig. 2d)<sup>41-51</sup>. Notably, the homogeneous control for the full reaction failed to produce any product.

## 3 Monolayered MOFs for photocatalytic organic transformations

The tunability of MOLs enables the design of MOL-based catalysts for other photocatalytic reactions. Recent advancements in

photoredox catalysis, which involve dual catalytic cycles utilizing a photosensitizer and a secondary catalytic center, have enabled unique organic transformations that are not readily accessible with ground-state catalysts<sup>52, 53</sup>. Moreover, earth-abundant metals, such as cobalt<sup>54</sup>, nickel<sup>55</sup>, and copper<sup>56</sup>, have proven effective in various photoredox-catalyzed cross-coupling reactions, offering a sustainable alternative to noble metals typically required for these reactions.

Photocatalytic systems built with MOLs can pre-organize photosensitizers and secondary catalysts, thereby accelerating electron transfer between them and significantly reducing the required catalyst loadings. Furthermore, MOL-based catalysts exhibit stability under various catalytic conditions, enabling their recycling and reuse, which further contributes to a more sustainable photocatalytic process.

Fig. 3 summarizes a variety of reactions accomplished by MOL-based photocatalysts and compares their efficiencies to those of corresponding homogeneous catalysts. Reactions **3a–3d** exemplify the synergy between photosensitizers and organocatalysts, including combinations of Ir-PS with Lewis acid (LA) assisted by stoichiometric amount of reductant<sup>57</sup> or oxidant<sup>58</sup>, Eosin Y (EY) with LA<sup>59</sup>, and pyridine (Py) nucleophiles<sup>60</sup>.



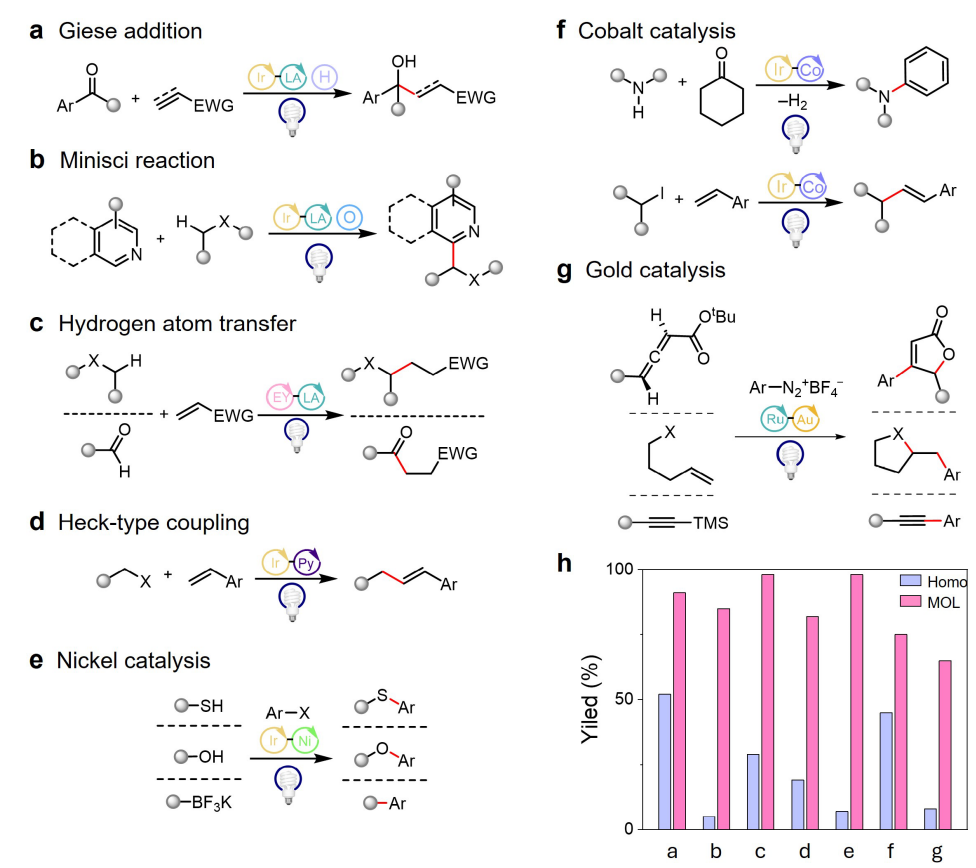


Fig. 3. A summary of photoredox reactions with MOL-based catalysts. a–g, Ene-carbonyl reduction coupling reaction (a), Minisci reaction (b), Giess addition mediated by hydrogen atom transfer (c), radical dehydrogenative coupling reaction of alkyl halides with styrene derivatives (d), Ni-catalyzed C–S, C–O, and C–C coupling reactions of aryl halides (e), Co-catalyzed dehydrogenative coupling reactions (photochemical aniline synthesis and radical Heck-type coupling reaction) (f), and gold-catalyzed arylation of C–C unsaturated bonds (g). The catalysts in the MOLs are shown as circles connected by a black line. h, Yields of MOL-catalyzed reactions (MOL, pink columns) and homogeneously catalyzed reactions (Homo, purple columns) at the same catalyst loadings.

In reaction 3a, for example, the MOL catalyst was prepared from HfCl<sub>4</sub> and Ir-PS ligands, and subsequently treated with trimethylsilyl triflate (TMSOTf) to introduce strongly Lewis acidic surface sites through post-modification. These Lewis acidic Hf sites effectively bind and activate electron-deficient alkenes, facilitating their interaction with ketyl radicals generated by adjacent Ir-PSs. This configuration suppresses undesired dimerization, thereby improving the selectivity for cross-coupling products by nine times. A stoichiometric amount of reductant, Hantzsch ester, was added to turnover the reaction.

Reactions **3e–3g** illustrate the synergy between photosensitizers and transition-metal catalysts, featuring combinations of Ir-PS with a Ni(bipyridine) complex<sup>61</sup>, Ir-PS with (pyridine)cobaloxime<sup>62</sup>, and Ru-based photosensitizer (Ru-PS) with a gold phosphine complex<sup>63</sup>.

In reaction 3e, for example, the MOL catalyst was constructed from Ir-PS ligands and then treated with Ni(MBA)Cl<sub>2</sub> [MBA = 2-(4'-methyl-[2,2'-bipyridin]-4-yl)acetate] to incorporate the Ni(bipyridine) complex through post-modification. The proximity between photosensitizing Ir centers and catalytic Ni centers (~ 0.85 nm) facilitates single electron transfer, leading to a 15-fold increase in photoredox reactivity. The MOL proves highly effectiveness in catalytic C–S, C–O, and C–C cross-coupling reactions with broad substrate scopes and turnover numbers of up to 4500, 1900, and 450, respectively.

As shown in Fig. 3, MOLs enhance these reactions to varying extents, with the highest enhancement being 15-folds in reaction 3e and the lowest of 1.7-folds in reaction 3f. These variations suggest different roles of photoelectron transfer in the reaction kinetics of these transformations. Understanding the kinetics of each step in the reaction cycle is crucial for designing efficient photocatalytic systems. In reaction 3e, photoelectron transfer either reduces Ni(II) to Ni(0) to facilitate oxidative addition or oxidizes Ni(II) aryl complexes coordinated with S, O, or C-based nucleophiles to Ni(III) to promote reductive elimination. These steps are rate-limiting. Consequently, pre-organization of dual catalytic sites in the MOL significantly boosts the reaction yield. Conversely, in reaction 3f, the electron transfer between the photosensitizer and the (pyridine)cobaloxime complex occurs rapidly and does not significantly affect the overall reaction rate.

While these reactions were studied based on literature precedents of homogeneous catalyses  $^{54}$ ,  $^{64-69}$ , reactions  $\bf 3a$  and  $\bf 3d$  are particularly noteworthy because achieving a high reaction yield with the same components in a homogeneous solution is challenging. As previously discussed, reaction  $\bf 3a$  competes with a side reaction, pinacol coupling. The installation of Lewis acid sites near the photosensitizer increases the local concentration of substrates, thereby improving reaction selectivity. Reaction  $\bf 3e$  involves sequential  $\bf S_N 2$  reaction (forming the pyridinium salt *in-situ* with the pyridine catalyst and the alkyl halide substrate), single electron



reduction, and radical dissociation (from the pyridinium salt). The  $S_{\rm N}2$  reaction and the radical dissociation, however, have opposite steric requirements on pyridine structures  $^{70}$ . Pre-organizing the pyridine and the photosensitizer in the MOL accelerates single electron reduction and radical dissociation steps, overcoming their reliance on ortho-substituted pyridine structures and allowing the use of non-substituted pyridines, which favors the  $S_{\rm N}2$  reaction. This method tolerates a broader range of substrates and enhances reaction efficiency.

The sustainability of MOL-catalyzed reactions is further bolstered by the ease of catalyst reuse (Fig. 4). For instance, MOL-catalyzed reaction 3f has been successfully applied in eight consecutive rounds of vesnarinone synthesis without loss of reactivities. After each reaction run, the well-dispersed material was recovered from the reaction mixture by centrifugation. The MOL was then washed and directly reused in the next reaction cycle. The PXRD pattern of the recovered MOL matched that of the assynthesized material, demonstrating the durability of MOL catalysts under catalytic conditions. This recycling procedure was also applied to the other reactions listed in Fig. 3.

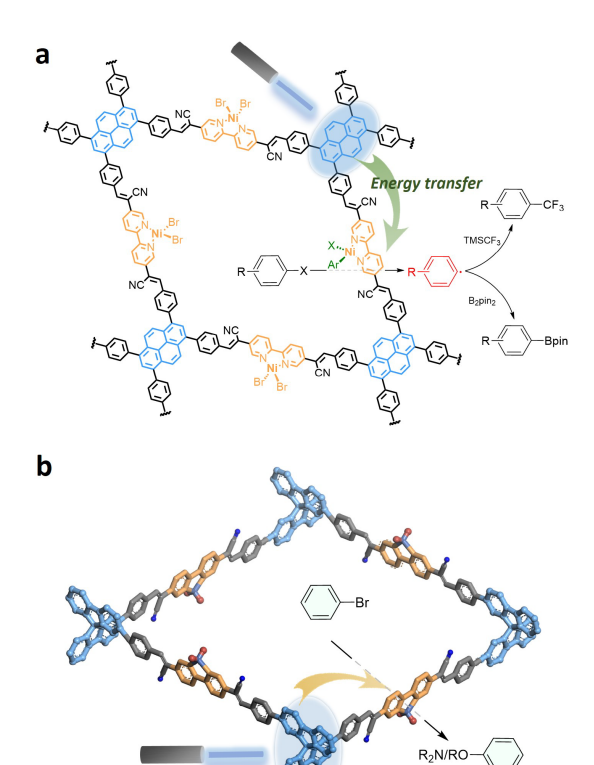


Fig. 4. MOL catalyst reuse for photochemical aniline synthesis.

### 4 COFs for photocatalytic organic transformations

The design principles of MOL-based photocatalysts can be adapted for designing COF-based photocatalysts. Recent studies have investigated the use of COFs in photoredox cross-coupling reactions to form C–C, C–N, C–O, and C–S bonds<sup>71–74</sup>. We hypothesize that pre-organizing photosensitizers and transition metal complexes in COFs will significantly enhance photocatalytic efficiency, potentially allowing the use of less reactive yet more sustainable organic photosensitizers in place of noble metal-based photosensitizers. Additionally, most reported COFs to date are two-dimensional systems with in-plane conjugation, a result of the use of  $\pi$ - $\pi$  interactions in driving COF synthesis. By modifying the conjugation structures, the photosensitizing properties of COFs can be tuned, potentially improving their efficiency for photocatalytic applications.

In this section, we discuss two COFs, one planar and one non-planar, both incorporating photosensitizers and Ni-bipyridine complexes (Fig. 5)<sup>75, 76</sup>. The planar COF, containing a pyrene chromophore and a Ni-bipyridine, shows high reactivity in radical borylation and trifluoromethylation reactions of aryl halides. This is attributed to the efficient in-plane energy transfer from the pyrene to the Ni-aryl intermediate upon irradiation<sup>77</sup>. On the other hand, the non-planar COF, featuring a spirobifluorenyl chromophore and a Ni-bipyridine, efficiently catalyzes photoredox C–N and C–O coupling reactions<sup>78, 79</sup>. Both COFs exhibit enhanced reactivities compared to their homogeneous counterparts, with the planar COF



**Fig. 5.** Two COFs for photocatalytic organic transformations. **a**, Planar COF for energy transfer catalysis. **b**, Non-planar COF for photoredox catalysis. Reproduced with permission from Ref.<sup>75</sup>, © Wiley 2023 and Ref.<sup>76</sup>, © American Chemical Society 2023.

Photoredox catalysis

showing a 2.7-fold improvement and the non-planar COF showing a 23-fold improvement.

The reactivity difference between the two COFs can be intuitively attributed to their difference in conjugation. The planar COF has strong conjugation, facilitating rapid exciton diffusion and benefiting energy transfer, while the non-planar COF with less efficient conjugation slows excited-state quenching. Additionally, the photoredox properties of pyrene and spirobifluorene differ. Spirobifluorene possesses strong photooxidation power that favors electron transfer in the reaction instead of energy transfer.

#### 5 Conclusions

Framework materials provide an ideal platform for designing photocatalytic systems with precise molecular control. Mimicking natural photosynthesis, pre-organization of photosensitizers and catalytic centers in framework materials significantly enhance the overall reaction efficiency. Successful demonstrations of the strategy in artificial photosynthesis and photoredox reactions have been achieved at the laboratory scale. Owing to the pre-organization of functional units in framework materials, their reaction kinetics can be significantly improved when photo-initiated electron or energy transfer becomes the rate-limiting step. Additionally, competing side reactions of photo-generated radicals are suppressed by substrate pre-organization in framework materials. Furthermore, recyclability of the framework materials and use of non-noble metal-based photosensitizers in the materials contribute to sustainability of these photocatalytic processes.

While scaling up the reactions discussed in this minireview may





pose challenges, the fundamental principles learnt in these examples will benefit the design of other photocatalytic systems aimed at achieving high-efficiency sustainable photocatalysis. Besides developing photocatalysts with longer excited state lifetimes (or hole-electron separation efficiency), integration of a co-catalyst that rapidly consumes the exciton offers an alternative method to enhance photocatalytic efficiency.

#### References

- Ballif, C.; Haug, F. J.; Boccard, M.; Verlinden, P. J.; Hahn, G. Status and perspectives of crystalline silicon photovoltaics in research and industry. *Nat. Rev. Mater.* 2022, 7, 597–616.
- [2] Hill, R.; Bendall, F. Function of the two cytochrome components in chloroplasts: A working hypothesis. *Nature* 1960, 186, 136–137.
- [3] Govindjee; Shevela, D.; Björn, L. O. Evolution of the Z-scheme of photosynthesis: A perspective. *Photosynth. Res.* 2017, 133, 5–15.
- [4] Balzani, V.; Moggi, L.; Manfrin, M. F.; Bolletta, F.; Gleria, M. Solar energy conversion by water photodissociation. *Science* 1975, 189, 852–856.
- [5] Lehn, J. M.; Ziessel, R. Photochemical generation of carbon monoxide and hydrogen by reduction of carbon dioxide and water under visible light irradiation. *Proc. Natl. Acad. Sci. USA* 1982, 79, 701–704.
- [6] Eckenhoff, W. T. Molecular catalysts of Co, Ni, Fe, and Mo for hydrogen generation in artificial photosynthetic systems. *Coord. Chem. Rev.* 2018, 373, 295–316.
- [7] Takeda, H.; Cometto, C.; Ishitani, O.; Robert, M. Electrons, photons, protons and earth-abundant metal complexes for molecular catalysis of CO<sub>2</sub> reduction. ACS Catal. 2017, 7, 70–88.
- [8] Marcus, R. A. On the theory of oxidation-reduction reactions involving electron transfer. I. J. Chem. Phys. 1956, 24, 966–978.
- [9] Kumagai, H.; Tamaki, Y.; Ishitani, O. Photocatalytic systems for CO<sub>2</sub> reduction: Metal-complex photocatalysts and their hybrids with photofunctional solid materials. Acc. Chem. Res. 2022, 55, 978–990.
- [10] Takata, T.; Jiang, J. Z.; Sakata, Y.; Nakabayashi, M.; Shibata, N.; Nandal, V.; Seki, K.; Hisatomi, T.; Domen, K. Photocatalytic water splitting with a quantum efficiency of almost unity. *Nature* 2020, 581, 411–414.
- [11] Nocera, D. G. The artificial leaf. Acc. Chem. Res. 2012, 45, 767-776.
- [12] Smith, P. T.; Nichols, E. M.; Cao, Z.; Chang, C. J. Hybrid catalysts for artificial photosynthesis: Merging approaches from molecular, materials, and biological catalysis. Acc. Chem. Res. 2020, 53, 575–587.
- [13] Chen, R.; Zhuang, G. L.; Wang, Z. Y.; Gao, Y. J.; Li, Z.; Wang, C.; Zhou, Y.; Du, M. H.; Zeng, S. Y.; Long, L. S. et al. Integration of bio-inspired lanthanide-transition metal cluster and P-doped carbon nitride for efficient photocatalytic overall water splitting. *Nat. Sci. Rev.* 2021, 8, nwaa234.
- [14] Yaghi, O. M.; Li, H. L. Hydrothermal synthesis of a metal-organic framework containing large rectangular channels. *J. Am. Chem. Soc.* 1995, 117, 10401–10402.
- [15] Côté, A. P.; Benin, A. I.; Ockwig, N. W.; O'Keeffe, M.; Matzger, A. J.; Yaghi, O. M. Porous, crystalline, covalent organic frameworks. *Science* 2005, 310, 1166–1170.
- [16] Yin, H. Q.; Zhang, Z. M.; Lu, T. B. Ordered integration and heterogenization of catalysts and photosensitizers in metal-/covalent organic frameworks for boosting CO<sub>2</sub> photoreduction. *Acc. Chem. Res.* 2023, 56, 2676–2687.
- [17] Pan, Z. H.; Weng, Z. Z.; Kong, X. J.; Long, L. S.; Zheng, L. S. Lanthanide-containing clusters for catalytic water splitting and CO<sub>2</sub> conversion. *Coord. Chem. Rev.* 2022, 457, 214419.
- [18] Drake, T.; Ji, P. F.; Lin, W. B. Site isolation in metal-organic frameworks enables novel transition metal catalysis. *Acc. Chem. Res.* 2018, 51, 2129–2138.
- [19] Kesanli, B.; Lin, W. B. Chiral porous coordination networks: Rational

- design and applications in enantioselective processes. *Coord. Chem. Rev.* **2003**, *246*, 305–326.
- [20] Lin, J. X.; Ouyang, J.; Liu, T. Y.; Li, F. X.; Sung, H. H. Y.; Williams, I.; Quan, Y. J. Metal-organic framework boosts heterogeneous electron donor-acceptor catalysis. *Nat. Commun.* 2023, 14, 7757.
- [21] Cheng, S. X.; Ouyang, J.; Li, M. Q.; Diao, Y. X.; Yao, J. C.; Li, F. X.; Lee, Y. F.; Sung, H. H. Y.; Williams, I.; Xu, Z. T. et al. Charge separation in metal-organic framework enables heterogeneous thiol catalysis. *Angew. Chem., Int. Ed.* 2023, 62, e202300993.
- [22] Feng, X. Y.; Song, Y.; Lin, W. B. Transforming hydroxide-containing metal-organic framework nodes for transition metal catalysis. *Trends Chem.* 2020, 2, 965–979.
- [23] Guo, S.; Kong, L. H.; Wang, P.; Yao, S.; Lu, T. B.; Zhang, Z. M. Switching excited state distribution of metal-organic framework for dramatically boosting photocatalysis. *Angew. Chem., Int. Ed.* 2022, 61, e202206193.
- [24] Zeng, L. Z.; Cao, Y. H.; Li, Z.; Dai, Y. H.; Wang, Y. K.; An, B.; Zhang, J. Z.; Li, H.; Zhou, Y.; Lin, W. B. et al. Multiple cuprous centers supported on a titanium-based metal-organic framework catalyze CO<sub>2</sub> hydrogenation to ethylene. ACS Catal. 2021, 11, 11696–11705.
- [25] Zhang, J. Z.; An, B.; Li, Z.; Cao, Y. H.; Dai, Y. H.; Wang, W. Y.; Zeng, L. Z.; Lin, W. B.; Wang, C. Neighboring Zn–Zr sites in a metalorganic framework for CO<sub>2</sub> hydrogenation. *J. Am. Chem.Soc.* 2021, 143, 8829–8837.
- [26] Jiang, J. C.; Gándara, F.; Zhang, Y. B.; Na, K.; Yaghi, O. M.; Klemperer, W. G. Superacidity in sulfated metal-organic framework-808. J. Am. Chem. Soc. 2014, 136, 12844–12847.
- [27] Cao, L. Y.; Lin, Z. K.; Peng, F.; Wang, W. W.; Huang, R. Y.; Wang, C.; Yan, J. W.; Liang, J.; Zhang, Z. M.; Zhang, T. et al. Self-supporting metal-organic layers as single-site solid catalysts. *Angew. Chem., Int. Ed.* 2016, 55, 4962–4966.
- [28] Jati, A.; Dey, K.; Nurhuda, M.; Addicoat, M. A.; Banerjee, R.; Maji, B. Dual metalation in a two-dimensional covalent organic framework for photocatalytic C-N cross-coupling reactions. *J. Am. Chem. Soc.* 2022, 144, 7822–7833.
- [29] Wang, H.; Wang, H.; Wang, Z. W.; Tang, L.; Zeng, G. M.; Xu, P.; Chen, M.; Xiong, T.; Zhou, C. Y.; Li, X. Y. et al. Covalent organic framework photocatalysts: Structures and applications. *Chem. Soc. Rev.* 2020, 49, 4135–4165.
- [30] Li, Z. P.; Zhi, Y. F.; Shao, P. P.; Xia, H.; Li, G. S.; Feng, X.; Chen, X.; Shi, Z.; Liu, X. M. Covalent organic framework as an efficient, metal-free, heterogeneous photocatalyst for organic transformations under visible light. *Appl. Catal. B: Environ.* 2019, 245, 334–342.
- [31] Xu, H. T.; Xia, S. L.; Li, C. L.; Li, Y.; Xing, W. D.; Jiang, Y.; Chen, X. Programming tetrathiafulvalene-based covalent organic frameworks for promoted photoinduced molecular oxygen activation. Angew. Chem., Int. Ed. 2024, 63, e202405476.
- [32] Liu, C.; Colón, B. C.; Ziesack, M.; Silver, P. A.; Nocera, D. G. Water splitting-biosynthetic system with CO<sub>2</sub> reduction efficiencies exceeding photosynthesis. *Science* 2016, 352, 1210–1213.
- [33] Hong, Y. H.; Lee, Y. M.; Nam, W.; Fukuzumi, S. Molecular photocatalytic water splitting by mimicking photosystems I and II. J. Am. Chem. Soc. 2022, 144, 695–700.
- [34] Wu, J. J. X.; Wang, X. Y.; Wang, Q.; Lou, Z. P.; Li, S. R.; Zhu, Y. Y.; Qin, L.; Wei, H. Nanomaterials with enzyme-like characteristics (nanozymes): Next-generation artificial enzymes (II). *Chem. Soc. Rev.* 2019, 48, 1004–1076.
- [35] Zhang, B. B.; Sun, L. C. Artificial photosynthesis: Opportunities and challenges of molecular catalysts. *Chem. Soc. Rev.* 2019, 48, 2216–2264.
- [36] Wang, Z.; Li, C.; Domen, K. Recent developments in heterogeneous photocatalysts for solar-driven overall water splitting. *Chem. Soc. Rev.* 2019, 48, 2109–2125.
- [37] Wang, S. B.; Wang, X. C. Multifunctional metal-organic frameworks for photocatalysis. *Small* 2015, 11, 3097–3112.





- [38] Wang, S. B.; Yao, W. S.; Lin, J. L.; Ding, Z. X.; Wang, X. C. Cobalt imidazolate metal-organic frameworks photosplit CO<sub>2</sub> under mild reaction conditions. *Angew Chem.*, Int. Ed. 2014, 53, 1034–1038.
- [39] Wang, S. B.; Wang, X. C. Photocatalytic CO<sub>2</sub> reduction by CdS promoted with a zeolitic imidazolate framework. *Appl. Catal. B: Environ.* 2015, 162, 494–500.
- [40] Lan, G. X.; Fan, Y. J.; Shi, W. J.; You, E.; Veroneau, S. S.; Lin, W. B. Biomimetic active sites on monolayered metal-organic frameworks for artificial photosynthesis. *Nat. Catal.* 2022, 5, 1006–1018.
- [41] Jiang, Z. F.; Wan, W. M.; Li, H. M.; Yuan, S. Q.; Zhao, H. J.; Wong, P. K. A hierarchical Z-scheme α-Fe<sub>2</sub>O<sub>3</sub>/g-C<sub>3</sub>N<sub>4</sub> hybrid for enhanced photocatalytic CO<sub>2</sub> reduction. *Adv. Mater.* 2018, 30, 1706108.
- [42] Wang, J. S.; Qin, C. L.; Wang, H. J.; Chu, M. N.; Zada, A.; Zhang, X. L.; Li, J. D.; Raziq, F.; Qu, Y.; Jing, L. Q. Exceptional photocatalytic activities for CO<sub>2</sub> conversion on Al–O bridged g-C<sub>3</sub>N<sub>4</sub>/α-Fe<sub>2</sub>O<sub>3</sub> Z-scheme nanocomposites and mechanism insight with isotopesZ. *Appl. Catal. B: Environ.* 2018, 221, 459–466.
- [43] Bae, K. L.; Kim, J.; Lim, C. K.; Nam, K. M.; Song, H. Colloidal zinc oxide-copper(I) oxide nanocatalysts for selective aqueous photocatalytic carbon dioxide conversion into methane. *Nat. Commun.* 2017, 8, 1156.
- [44] Jin, J.; Yu, J. G.; Guo, D. P.; Cui, C.; Ho, W. A hierarchical Z-scheme CdS-WO<sub>3</sub> photocatalyst with enhanced CO<sub>2</sub> reduction activity. *Small* 2015. 11, 5262–5271.
- [45] Aguirre, M. E.; Zhou, R. X.; Eugene, A. J.; Guzman, M. I.; Grela, M. A. Cu<sub>2</sub>O/TiO<sub>2</sub> heterostructures for CO<sub>2</sub> reduction through a direct Z-scheme: Protecting Cu<sub>2</sub>O from photocorrosion. *Appl. Catal. B: Environ.* 2017, 217, 485–493.
- [46] Shen, Y.; Han, Q. T.; Hu, J. Q.; Gao, W.; Wang, L.; Yang, L. Q.; Gao, C.; Shen, Q.; Wu, C. P.; Wang, X. Y. et al. Artificial trees for artificial photosynthesis: Construction of dendrite-structured α-Fe<sub>2</sub>O<sub>3</sub>/g-C<sub>3</sub>N<sub>4</sub> Z-scheme system for efficient CO<sub>2</sub> reduction into solar fuels. ACS Appl. Energy Mater. 2020, 3, 6561–6572.
- [47] Han, Q. T.; Li, L.; Gao, W.; Shen, Y.; Wang, L.; Zhang, Y. T.; Wang, X. Y.; Shen, Q.; Xiong, Y. J.; Zhou, Y. et al. Elegant construction of ZnIn<sub>2</sub>S<sub>4</sub>/BiVO<sub>4</sub> hierarchical heterostructures as direct Z-scheme photocatalysts for efficient CO<sub>2</sub> photoreduction. ACS Appl. Mater. Interfaces 2021, 13, 15092–15100.
- [48] Guo, R. T.; Liu, X. Y.; Qin, H.; Wang, Z. Y.; Shi, X.; Pan, W. G.; Fu, Z. G.; Tang, J. Y.; Jia, P. Y.; Miao, Y. F. et al. Photocatalytic reduction of CO<sub>2</sub> into CO over nanostructure Bi<sub>2</sub>S<sub>3</sub> quantum dots/g-C<sub>3</sub>N<sub>4</sub> composites with Z-scheme mechanism. *Appl Surf. Sci.* 2020, 500, 144059.
- [49] Jiang, Z.; Xu, X. H.; Ma, Y. H.; Cho, H. S.; Ding, D.; Wang, C.; Wu, J.; Oleynikov, P.; Jia, M.; Cheng, J. et al. Filling metal-organic framework mesopores with TiO<sub>2</sub> for CO<sub>2</sub> photoreduction. *Nature* 2020, 586, 549–554
- [50] Liang, L.; Li, X. D.; Sun, Y. F.; Tan, Y. L.; Jiao, X. C.; Ju, H. X.; Qi, Z. M.; Zhu, J. F.; Xie, Y. Infrared light-driven CO<sub>2</sub> overall splitting at room temperature. *Joule* 2018, 2, 1004–1016.
- [51] Wu, L. Y.; Mu, Y. F.; Guo, X. X.; Zhang, W.; Zhang, Z. M.; Zhang, M.; Lu, T. B. Encapsulating perovskite quantum dots in iron-based metal-organic frameworks (MOFs) for efficient photocatalytic CO<sub>2</sub> reduction. *Angew. Chem., Int. Ed.* 2019, 58, 9491–9495.
- [52] Shaw, M. H.; Twilton, J.; MacMillan, D. W. C. Photoredox catalysis in organic chemistry. J. Org. Chem. 2016, 81, 6898–6926.
- [53] Romero, N. A.; Nicewicz, D. A. Organic photoredox catalysis. *Chem. Rev.* 2016, 116, 10075–10166.
- [54] Dighe, S. U.; Juliá, F.; Luridiana, A.; Douglas, J. J.; Leonori, D. A photochemical dehydrogenative strategy for aniline synthesis. *Nature* 2020, 584, 75–81.
- [55] Zuo, Z. W.; Ahneman, D. T.; Chu, L. L.; Terrett, J. A.; Doyle, A. G.; MacMillan, D. W. C. Merging photoredox with nickel catalysis: Coupling of α-carboxyl sp³-carbons with aryl halides. *Science* 2014, 345, 437–440.
- [56] Kautzky, J. A.; Wang, T.; Evans, R. W.; MacMillan, D. W. C.

- Decarboxylative trifluoromethylation of aliphatic carboxylic acids. J. Am. Chem. Soc. 2018, 140, 6522–6526.
- [57] Fan, Y. J.; You, E.; Xu, Z. W.; Lin, W. B. A substrate-binding metalorganic layer selectively catalyzes photoredox ene-carbonyl reductive coupling reactions. J. Am. Chem. Soc. 2021, 143, 18871–18876.
- [58] Quan, Y. J.; Lan, G. X.; Fan, Y. J.; Shi, W. J.; You, E.; Lin, W. B. Metal-organic layers for synergistic Lewis acid and photoredox catalysis. J. Am. Chem. Soc. 2020, 142, 1746–1751.
- [59] Zheng, H. F.; Fan, Y. J.; Blenko, A. L.; Lin, W. B. Sequential modifications of metal-organic layer nodes for highly efficient photocatalyzed hydrogen atom transfer. J. Am. Chem. Soc. 2023, 145, 9994–10000.
- [60] Fan, Y. J.; Blenko, A. L.; Labalme, S.; Lin, W. B. Metal-organic layers with photosensitizer and pyridine pairs activate alkyl halides for photocatalytic heck-type coupling with olefins. *J. Am. Chem. Soc.* 2024, 146, 7936–7941.
- [61] Lan, G. X.; Quan, Y. J.; Wang, M. L.; Nash, G. T.; You, E.; Song, Y.; Veroneau, S. S.; Jiang, X. M.; Lin, W. B. Metal-organic layers as multifunctional two-dimensional nanomaterials for enhanced photoredox catalysis. J. Am. Chem. Soc. 2019, 141, 15767–15772.
- [62] Fan, Y. J.; Zheng, H. F.; Labalme, S.; Lin, W. B. Molecular engineering of metal-organic layers for sustainable tandem and synergistic photocatalysis. J. Am. Chem. Soc. 2023, 145, 4158–4165.
- [63] Zheng, H. F.; Fan, Y. J.; Song, Y.; Chen, J. S.; You, E.; Labalme, S.; Lin, W. B. Site isolation in metal-organic layers enhances photoredox gold catalysis. J. Am. Chem. Soc. 2022, 144, 10694–10699.
- [64] Lee, K. N.; Lei, Z.; Ngai, M. Y. β-selective reductive coupling of alkenylpyridines with aldehydes and imines via synergistic Lewis acid/photoredox catalysis. J. Am. Chem. Soc. 2017, 139, 5003–5006.
- [65] Jin, J.; MacMillan, D. W. C. Direct α-Arylation of ethers through the combination of photoredox-mediated C–H functionalization and the minisci reaction. *Angew. Chem., Int. Ed.* 2015, 54, 1565–1569.
- [66] Fan, X. Z.; Rong, J. W.; Wu, H. L.; Zhou, Q.; Deng, H. P.; Tan, J. D.; Xue, C. W.; Wu, L. Z.; Tao, H. R.; Wu, J. Eosin Y as a direct hydrogen-atom transfer photocatalyst for the functionalization of C-H bonds. *Angew. Chem.*, *Int. Ed.* 2018, 57, 8514–8518.
- [67] Liu, Q.; Yi, H.; Liu, J.; Yang, Y. H.; Zhang, X.; Zeng, Z. Q.; Lei, A. W. Visible-light photocatalytic radical alkenylation of α-carbonyl alkyl bromides and benzyl bromides. *Chem.- European J.* 2013, 19, 5120–5126.
- [68] Oderinde, M. S.; Frenette, M.; Robbins, D. W.; Aquila, B.; Johannes, J. W. Photoredox mediated nickel catalyzed cross-coupling of thiols with aryl and heteroaryl iodides via thiyl radicals. *J. Am. Chem. Soc.* 2016, 138, 1760–1763.
- [69] Sahoo, B.; Hopkinson, M. N.; Glorius, F. Combining gold and photoredox catalysis: Visible light-mediated oxy- and aminoarylation of alkenes. J. Am. Chem. Soc. 2013, 135, 5505–5508.
- [70] Tcyrulnikov, S.; Cai, Q. Q.; Twitty, J. C.; Xu, J. Y.; Atifi, A.; Bercher, O. P.; Yap, G. P. A.; Rosenthal, J.; Watson, M. P.; Kozlowski, M. C. Dissection of alkylpyridinium structures to understand deamination reactions. ACS Catal. 2021, 11, 8456–8466.
- [71] Traxler, M.; Gisbertz, S.; Pachfule, P.; Schmidt, J.; Roeser, J.; Reischauer, S.; Rabeah, J.; Pieber, B.; Thomas, A. Acridinefunctionalized covalent organic frameworks (COFs) as photocatalysts for metallaphotocatalytic C-N cross-coupling. *Angew. Chem., Int. Ed.* 2022, 61, e202117738.
- [72] Dong, W. B.; Yang, Y.; Xiang, Y. G.; Wang, S. Y.; Wang, P.; Hu, J. X.; Rao, L.; Chen, H. A highly stable all-in-one photocatalyst for aryl etherification: The Ni<sup>II</sup> embedded covalent organic framework. *Green Chem.* 2021, 23, 5797–5805.
- [73] Chen, H.; Liu, W. L.; Laemont, A.; Krishnaraj, C.; Feng, X.; Rohman, F.; Meledina, M.; Zhang, Q. Q.; Van Deun, R.; Leus, K. et al. A visible-light-harvesting covalent organic framework bearing single nickel sites as a highly efficient sulfur-carbon cross-coupling dual catalyst. *Angew. Chem., Int. Ed.* 2021, 60, 10820–10827.
- [74] López-Magano, A.; Ortín-Rubio, B.; Imaz, I.; Maspoch, D.; Alemán,



- J.; Mas-Ballesté, R. Photoredox heterobimetallic dual catalysis using engineered covalent organic frameworks. *ACS Catal.* **2021**, *11*, 12344–12354.
- [75] Fan, Y. J.; Kang, D. W.; Labalme, S.; Li, J. H.; Lin, W. B. Enhanced energy transfer in a π-conjugated covalent organic framework facilitates excited-state nickel catalysis. *Angew. Chem., Int. Ed.* 2023, 62, e202218908.
- [76] Fan, Y. J.; Kang, D. W.; Labalme, S.; Lin, W. B. A Spirobifluorene-based covalent organic framework for dual photoredox and nickel catalysis. J. Am. Chem. Soc. 2023, 145, 25074–25079.
- [77] Ting, S. I.; Garakyaraghi, S.; Taliaferro, C. M.; Shields, B. J.; Scholes, G. D.; Castellano, F. N.; Doyle, A. G. <sup>3</sup>d-d excited states of Ni(II) complexes relevant to photoredox catalysis: Spectroscopic identification and mechanistic implications. *J. Am. Chem. Soc.* 2020, 142, 5800–5810.
- [78] Terrett, J. A.; Cuthbertson, J. D.; Shurtleff, V. W.; MacMillan, D. W. C. Switching on elusive organometallic mechanisms with photoredox catalysis. *Nature* 2015, 524, 330–334.

[79] Corcoran, E. B.; Pirnot, M. T.; Lin, S. S.; Dreher, S. D.; DiRocco, D. A.; Davies, I. W.; Buchwald, S. L.; MacMillan, D. W. C. Aryl amination using ligand-free Ni(II) salts and photoredox catalysis. *Science* 2016, 353, 279–283.

#### **Acknowledgements**

We acknowledge the National Science Foundation (CHE-2102554) and the University of Chicago for funding support.

#### **Author contributions**

Y.F. prepared the manuscript draft. W.L. revised the manuscript.

#### Competing interests

The authors declare no competing interests.

Open Access This article is licensed under a Creative Commons Attribution 4.0 International License (CC BY 4.0), which permits reusers to distribute, remix, adapt, and build upon the material in any medium or format, so long as attribution is given to the original author(s) and the source, provide a link to the license, and indicate if changes were made. See https://creativecommons.org/licenses/by/4.0/

